Vol. 6, No.1, 2012 Chemistry

Sergey Kurta

CATALYSIS OF ETHYLENE OXYCHLORINATION INTO 1,2-DICHLORETHANE IN THE PRESENCE OF $CuCl_2$/CuCl ACTIVE CENTRES ON THE SURFACE OF g-Al_2O_3

Vasyl Stefanyk Precarpathian National University, Institute of Natural Science, 57, Shevchenko str., 76025 Ivano-Frankivsk, Ukraine; kca2007@mail.ru

Received: August 20, 2010 / Revised: December 12, 2010 / Accepted: March 03, 2011

© Kurta S., 2012

Abstract. The structure of $CuCl_2$, CuCl catalyst active centres on the surface of γ-Al_2O_3 has been investigated on the basis of X-ray diffraction analysis. The influence of the catalyst structure on the mechanism of ethylene oxidative chlorination has been determined. Using mass spectroscopy the difference in the structure of active centers and the mechanism of the deposited and impregnated types of $CuCl_2$, CuCl/γ-Al_2O_3 catalysts in the process of ethylene oxidative chlorination into 1,2-dichlorethane has been studied.

Keywords: process, catalyst, oxidative, chlorination, analysis, mass spectroscopy, X-ray diffraction, analysis, centres, mechanism, activity, productivity.

1. Introduction

1,2-dichlorethane (1,2-DCE) is obtained during the process of ethylene oxidative chlorination (EOC) using the catalysts based on copper chlorides, deposited and impregnated on the surface of γ-Al_2O_3. Using the mentioned types of $CuCl_2$, CuCl/γ-Al_2O_3 catalysts the qualitative and quantitative composition of EOC products, as well as its mechanism, can be changed.

The EOC process is carried out in the catalyst fluidized bed at the temperature of 478–505 K and pressure of 0.25–0.4 MPa in the reaction zone [1].

The reaction of EOC into 1,2-DCE proceeds by the following summary reaction:

$$C_2H_4 + 2HCl + 0.5O_2 \rightarrow C_2H_4Cl_2 + H_2O + Q \quad (1)$$

At the same time the secondary reaction of ethylene burning takes place:

$$C_2H_4 + 3O_2 \rightarrow 2CO_2 + 2H_2O \quad (2)$$

M. Flid and Yu. Tregger [2] assert that the following processes involving copper catalysts occur:

$$2CuCl_2 + C_2H_4 \rightarrow C_2H_4Cl_2 + 2CuCl \quad (3)$$

$$2CuCl + O_2 \rightarrow Cu_2OCl_2 \quad (4)$$

$$Cu_2OCl_2 + 2HCl \rightarrow 2CuCl_2 + H_2O \quad (5)$$

But the interaction between γ-Al_2O_3 surface and copper chlorides [3] is not described in any work. It is well-known that copper chlorides without the support do not catalyze ethylene oxychlorination [4]. Therefore, to the authors mind [5], the description of EOC mechanism (Eqs.(3)-(5)) [3] without participation of γ-Al_2O_3 surface groups is inaccurate.

At the same time during EOC the by-reactions can occur forming the following products: carbon tetrachloride, chloral, chloroform, trichlorethane, trichloroethylene and other by-products, in the general amount of 1–2 % to calculate for the obtained 1,2-DCE [6].

2. Experimental

2.1. Materials

Five samples were compared: 1) pure γ-Al_2O_3, as a catalyst support; 2) X1 – $CuCl_2$ catalyst, deposited from muriatic aqueous solution on the surface of γ-Al_2O_3 in the amount of 5 % $Cu^{+2,+1}$ (produced by "Harshow" firm); 3) MEDC-B catalyst on the basis of γ-Al_2O_3, co-precipitated with $CuCl_2$ for all volume in the amount of 5 % $Cu^{+2,+1}$ (produced by "Montecatini" firm); 4) $CuCl_2 \cdot 2H_2O$ – crystalline hydrate of the catalyst main component [7]; 5) $CuCl_2 \cdot 2HCl$ – hydrochloride of the catalyst main component [7].

2.2. Methods

Surface compounds obtained on the samples were identified by the infrared spectroscopy with the help of THERMO NICOLET NEXUS FT-IR in the frequencies range of 4000–400 cm^{-1}, using add-on device of diffusive

reflection with a resolution of 4 and a scan number of 50. Samples in the powder form preliminary diluted with KBr [8] were used.

In order to determine the active centers structure thermografic investigations were carried out using Paulic-Paulic-Erday photoderivatograph in the temperature range of 298–1273 K according to the standard methods of the Institute of Chemistry of the National Academy of Sciences of Ukraine [9].

The diffraction patterns were obtained by means of the DRON-4-07 diffractometer using the Bragg-Brentano X-ray focusing. The anode copper emission was the most suitable for research (l = 1.54178 Å). A Ni-filter was used for the reflected rays. The goniometer rate was 1–2 degrees per minute. The sample was prepared by applying the powder on a petroleum butter layer (amorphous substance), which had been previously applied with a thin layer on a quartz cell.

For mass spectroscopy a monopole MX-7304A mass spectrometer (Ukraine) was used with a mass range of 1–210, with the electron impact ionization, converted for thermal desorption measuring. A sample of 0.1–20 mg was placed at the bottom of a quartz-molybdenum ampoule and then the pressure was reduced to $5 \cdot 10^{-5}$ Pa. The heating rate was 0.15 K/s until 1023 K was achieved. Thermolysis volatile products were directed to the ionization chamber of the mass spectrometer, where they were ionized and fragmented under the influence of the electron impact. The mass spectra were recorded by the computer-aided automated data recording and processing system. The study of the temperature dependence of the desorption rate of thermal transformation products may provide information on the identification and the interaction energy of the copper chlorides active phase with the support surface [10].

3. Results and Discussion

3.1. X-ray Phase Analysis of the Support, Catalysts and Copper Chlorides Samples

For a more detailed study of investigated objects, the X-ray phase analysis of the support and the catalysts was carried out [11].

The diffractograms of the X1 catalyst samples (Fig. 1) differ from those of the initial γ-Al_2O_3 sample. These differences consist of a decrease of the intensity of diffraction patterns peaks by 25–27 % at 2θ in the range of 66.9°; 45.9°; 36.65°. This indicates the presence of other phases in the sample, namely $[CuCl_2]^{-1}$, $[CuCl_4]^{-2}$, which interact with the γ-Al_2O_3 surface groups and decrease their intensity. Furthermore, the above mentioned curve for the X1 catalyst sample shows a new peak of additional maximum in the area of 28.55° (Fig. 2). It can be identified as a new phase of pure $CuCl_2$ [15], yet the mentioned peaks do not coincide with the corresponding peaks of the diffraction pattern for pure $CuCl_2$. This suggests that copper chloride deposited by adsorption over γ-Al_2O_3 surface interacts with the surface alumina and hydroxyl groups 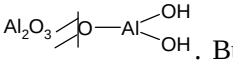 . But pure X1 catalyst (compared diffraction patterns 2 and 3 in Fig. 1), does not contain any copper hydroxychloride or contains very small quantity of it, which corresponds to the peaks in the area of 32.4°; 36.65°; 39.25°. After the X1 catalyst exposure to the air its diffraction pattern shows an additional peak at 16.1°, which is absent in the diffraction pattern of a pure sample (Fig. 1). This can be obviously explained by the formation of copper hydroxides and mixed hydroxychlorides Cu(OH)Cl or $Cu(OH)_2$ and $CuCl_2 \cdot 2H_2O$ due to water vapour in the air (Fig. 1) [12]. The study of diffraction patterns of the MEDC-B catalyst samples (Fig. 2) suggests the following: the same as for X1 catalyst, the application of copper chloride over γ-Al_2O_3 surface proportionally decreases the peak intensity in the area of 67°; 45.75° and 37.1° by 26–25 %. Such decrease indicates the presence of other phases $[CuCl_2]^{-1}$, $[CuCl_4]^{-2}$, Cu(OH)Cl, which interact with Al_2O_3 surface groups in the MEDC-B catalyst.

But in contrast to the X1 catalyst, the crystal form of $CuCl_2$ was not found in the area of 28.55° with MEDC-B (Fig. 2). It may be concluded that all active copper chloride is evenly distributed for all the volume of the MEDC-B catalyst particles and bounded with the Al_2O_3 surface.

On the basis of Tables 1 and 2 data, one can presume that the surface compounds structure of the catalyst $CuCl_2$ on the γ-Al_2O_3 support is different for the X1 and the MEDC-B catalyst samples. Judging from approximately equal values of peak intensity for the MEDC-B catalyst in the area of 32°, 37° i 39°, we can discuss the structure of surface compounds of the catalyst and the support, for example $[CuCl_2]Al(OH)_2$, $[CuCl_4]AlO$, $[CuCl_4]Al(OH)$, which were investigated by us earlier [11].

At the same time, for the X1 catalyst (Table 1, Fig. 1) the peak intensity in the area of 32°, 37° and 39° differs greatly. This indicates the presence on the X1 catalyst surface of at least three, maybe more, different compounds between $CuCl_2$ and γ-Al_2O_3, which is also confirmed by the available sources [12]. The data of Tables 1 and 2 which show the difference in interplanar spacing (Δd) for the catalyst support (d_{Al2O3}), the X1 catalyst (d_{X1}) (Table 1) and the MEDC-B catalyst ($d_{MEDC\text{-}B}$) (Table 2), suggest the following conclusions.

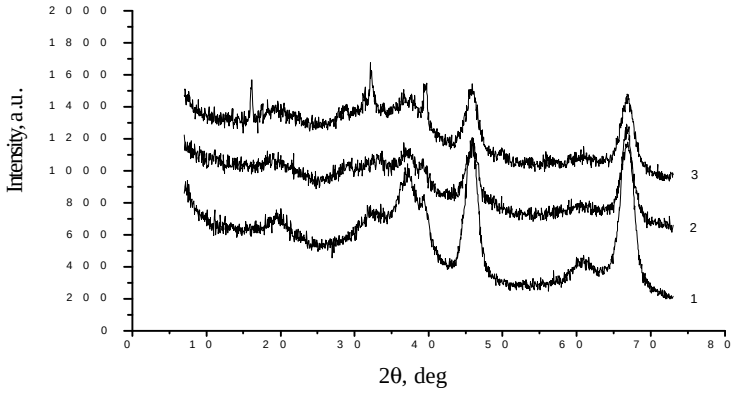

Fig. 1. Diffractograms of samples: γ-Al_2O_3 (1); X1 catalyst (2) and X1 catalyst after a few days of exposure to theair (3)

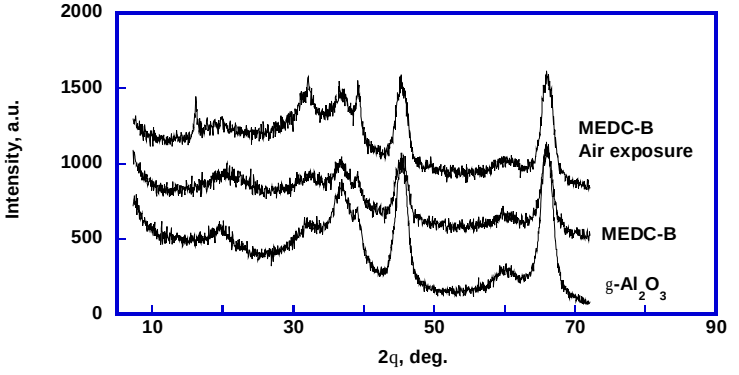

Fig. 2. Diffractograms of samples: γ-Al_2O_3 (1); MEDC-B catalyst (2) and MEDC-B catalyst after a few days of exposure to the air (3)

Table 1

Angular positions of diffraction lines 2q, corresponding interplanar spacing *d*, and relative intensity I/I_0, for the X1 catalyst

No.	2θ, °	Intensity *I*, s^{-1}	*d*, Å	I/I_0, %	$\Delta d = d_{X1}$-dAl_2O_3
1	18.95	1109	4.68293	87.5226	-
2	**19.7**	**1114**	**4.5063**	**88.42676**	**+0.0778**
3	21.75	1108	4.08599	87.34177	-
4	**28.55**	**1071**	**3.12638**	**80.65099**	**+3.1263**
5	29.6	1080	3.01783	82.27848	-
6	30.4	1069	2.94021	80.28933	-
7	31.45	1087	2.8444	83.5443	-
8	**32.4**	**1105**	**2.76314**	**86.79928**	**-0.0167**
9	33.7	1124	2.65946	90.23508	-
10	35.3	1080	2.5425	82.27848	-
11	**36.65**	**1175**	**2.45189**	**99.4575**	**+0.00318**
12	37.5	1141	2.39825	93.30922	-
13	**39.25**	**1074**	**2.29526**	**81.19349**	**+0.0056**
14	40.6	934	2.222	55.87703	-
15	43.15	895	2.09641	48.82459	-
16	**45.9**	**1209**	**1.97701**	**105.60579**	**+0.0060**
17	48.4	852	1.88057	41.04882	-
18	50.1	795	1.82068	30.74141	-
19	52.25	763	1.75071	24.95479	-
20	59.25	824	1.55949	35.98553	-
21	60.45	817	1.53138	34.71971	-
22	61.7	812	1.50332	33.81555	-
23	**66.9**	**1178**	**1.39854**	**100**	**-0.0027**

Table 2

Angular positions of diffraction lines 2θ, corresponding interplanar spacing *d*, and relative intensity I/I_0, for the MEDC-B catalyst

No.	2θ, °	Intensity *I*, s^{-1}	*d*, Å	I/I_0, %	$\Delta d = d_{MEDC-B}-d_{Al2O3}$
1	16.95	1092	5.23071	73.39901	-
2	**20.55**	**1150**	**4.32179**	**82.92282**	**-0.1066**
3	23.95	1111	3.71541	76.51888	-
4	**32.6**	**1098**	**2.74664**	**74.38424**	**-0.0332**
5	**37.1**	**1193**	**2.42318**	**89.98358**	**+0.0031**
6	**39.45**	**1094**	**2.28408**	**73.72742**	**-0.0055**
7	45.75	1219	1.98314	94.25287	+0.00122
8	60.5	860	1.53023	35.30378	-
9	**67**	**1254**	**1.3967**	**100**	**-0.0046**

The X1 catalyst, if compared to the γ-Al_2O_3 support, is characterized by an increase in the interplanar spacing for most of the characteristic peaks in the diffraction patterns in the areas of 28.55º; 36.55º; 39.25º; 45.9º; 79.7º, that indicates a wedging effect of the excess crystal phase of pure $CuCl_2$+CuCl [13]. In contrast, the MEDC-B catalyst, if compared to the γ-Al_2O_3 support, is characterized by a decrease in the interplanar spacing for most of the diffraction line peaks in the areas of 20.55º; 32.6º; 39.45º and 68.0º, that indicates phases homogeneity of the catalyst and the support, in which the catalyst is present both on the surface and in the structure and which has not pure crystal phase of $CuCl_2$.

3.2. Mass Spectrometry of the Support, Catalyst and Copper Chlorides Samples

The samples of the X1 and the MEDC-B catalysts, the γ-Al_2O_3 support and the $CuCl_2 \cdot H_2O$ and $CuCl_2 \cdot 2HCl$ or $H_2[CuCl_4]$ active phases were analyzed using the method of temperature-programmed desorption mass spectrometry for identifying of thermal transformation individual products on the surface of the catalysts, support and copper chlorides active phase. The mass spectrometry curves (Figs. 3–7) represent a qualitative and quantitative analysis of the compounds desorbed from the surface of the given objects.

As we predicted in our previous research using DTA and infrared spectroscopy [11], the maximum desorption of the physically bound water from the surface of the support (Fig. 3) and the catalysts (Figs. 4 and 5) takes place at the temperatures above 373 K, and they are identified by the molecular weight of water H_2O M_m = 16–18. Moreover, at the same curves one can identify small desorption peaks for carbon dioxide CO_2 M_m = 44, which are more typical for the support and less characteristic for the catalyst, with maximum desorption at the temperature close to 353 K. However, the situation with products desorbed from catalysts is much more complicated. For the X1 catalyst ethylene desorption is identified in the area of 373–423 K (M_m = 28), which is almost absent for the MEDC-B catalyst. But the main transformations on the catalyst surface start in the area of temperatures above 423 K. For the MEDC-B catalyst the maximum HCl loss (M_m = 35–38) is observed at 413 K, where several desorption curves belonging to HCl can be identified. The difference between them can be explained by different desorption rate of HCl of different origin from the catalyst surface, which can be the result of its release from different places on the catalyst surface and from its internal structure, or due to the decomposition of $CuCl_2 \cdot 2HCl$ or $H_2[CuCl_4]$ and $CuCl_2 \cdot H_2O$. At the same time, such similar HCl desorption curves for both catalysts are again observed at higher temperature. For the X1 catalyst this area corresponds to the desorption temperature of 733 K and for the MEDC-B catalyst the maximum is reached at 543 K. Obviously, it is this range of temperatures where the reaction of ethylene oxidative chlorination occurs – from 483 to 533 K for X1 and from 493 to 543 K for MEDC-B. Moreover, in this range one also observes the loss of water, which can be produced due to the reaction of $CuCl_2 \cdot H_2O$ dehydration [15].

We consider that dehydration and dehydrochlorination of the copper chlorides of the catalyst active phase occurs as represented in Eqs. (6)-(7). As the peak intensity of HCl loss in the range of 493–543 K on the MEDC-B catalyst (Fig. 4) is almost twice higher than that of the X1 catalyst (Fig. 5), one can presume more intensive proceeding of the reaction of ethylene oxidative chlorination with the impregnated catalyst of MEDC-B type. The analysis of the desorption curves of the $CuCl_2 \cdot H_2O$ (Fig. 6) and $CuCl_2 \cdot 2HCl$ or $H_2[CuCl_4]$ active phase (Fig. 7) suggests the following. In the temperature range from 373 to 473 K a partially hydrolyzed active phase of $CuCl_2 \cdot H_2O$ loses a very big amount of adsorbed and internally crystallization water; the release of crystallization water starts at the temperatures above 443 K and the release of adsorbed water – at the temperatures above 323 K, that is not observed with a pure active phase of $CuCl_2 \cdot 2HCl$ or $H_2[CuCl_4]$.

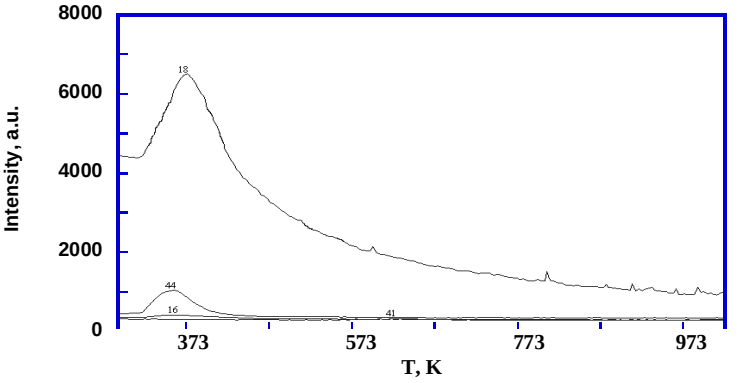

Fig. 3. Thermal desorption curves of the γ-Al_2O_3 carrier decomposition, obtained with the use of mass spectroscopy

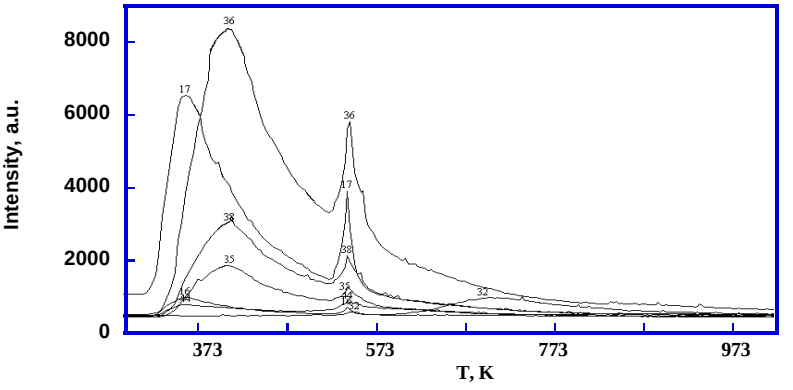

Fig. 4. Thermal desorption curves of the MEDC-B catalyst decomposition, obtained with the use of mass spectroscopy

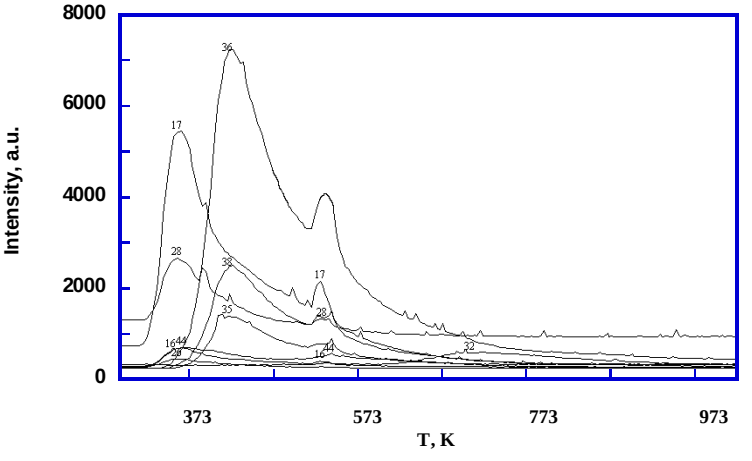

Fig. 5. Thermal desorption curves of the X1 catalyst decomposition, obtained with the use of mass spectroscopy

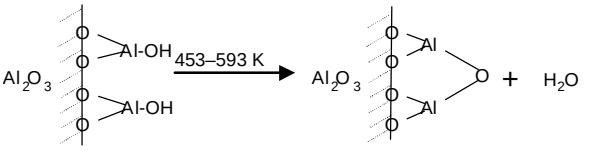

dehydration (6)

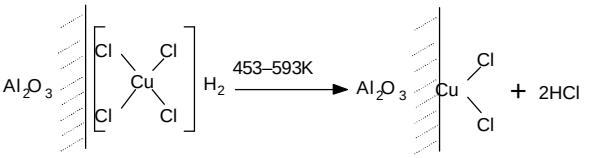

dechlorination (7)

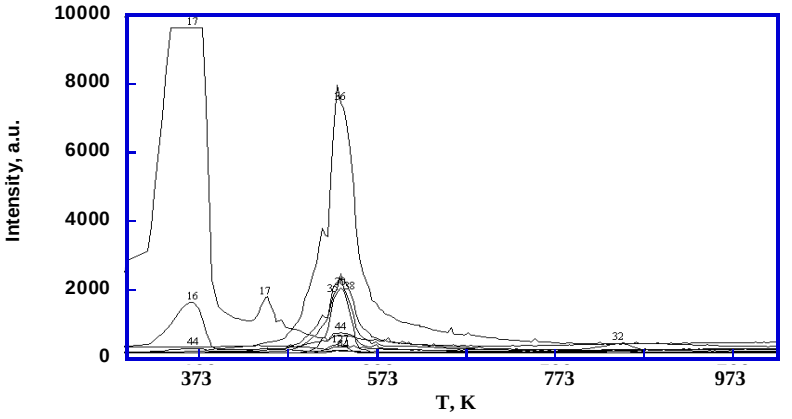

Fig. 6. Thermal desorption curves of the $CuCl_2 \cdot H_2O$ active phase decomposition, obtained with the use of mass spectroscopy

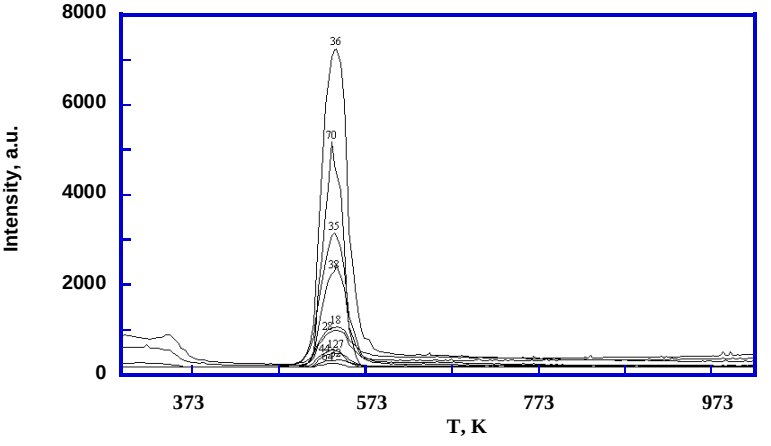

Fig. 7. Thermal desorption curves of the $CuCl_2 \cdot 2HCl$ or $H_2[CuCl_4]$ active phase decomposition, obtained with the use of mass spectroscopy

Intensive processes of dehydrochlorination of the $CuCl_2 \cdot H_2O$ active phase occur in the range of 473–573 K and are identified by maximum peaks of HCl desorption at 533 K for both types of active phase. But with a pure non-hydrolyzed phase of $CuCl_2 \cdot 2HCl$ or $H_2[CuCl_4]$, the intensity of dehydrochlorination processes is higher and consists of 3 peaks, whereas with a partially hydrolyzed $CuCl_2 \cdot H_2O$, it consists of only 2 peaks of HCl desorption (M_m = 35–38). But the most interesting characteristic of the desorption processes of active phase decomposition products is the occurrence of an intense peak of molecular chlorine Cl_2 desorption at 483–533 K (M_m = 70), which, in its turn, is two times more intense for a pure active phase of $H_2[CuCl_4]$. This phenomenon, never observed before with other methods of analysis, may be the evidence of active phase decomposition with the release of Cl_2 (Eqs. (8) and (9)), which may be involved in the chlorination of ethylene into 1,2-DCE [6].

$$H_2[CuCl_4] \xrightarrow{493\ K} H_2[CuCl_2] + 1/2Cl_2 + HCl \quad (8)$$

$$H_2[CuCl_4] \xrightarrow{508\ K} 2HCl + CuCl_2 \quad (9)$$

The available sources [16] describe similar phenomena of chlorine release from the catalyst active phase when the copper dichloride turns into the copper monochloride.

$$2CuCl_2 = 2CuCl + Cl_2 \quad (10)$$

Taking into account the above mentioned, we may confirm the structure of active centres on the surface of X1 and MEDC-B catalysts, as presented by us in [9]. Moreover, the release of HCl and Cl_2 (Eqs. (8)–(10)) in the processes of the active phase thermal destruction within the temperature range of 483–508 K of the EOC reaction confirms the mechanism of this reaction [17].

3.3. Predicted Mechanism of EOC Reactions on the Catalyst Surface

On the basis of X-ray phase analysis and electronic microscopy data described earlier [9] and the data of infrared spectroscopy and differential thermal analysis of the samples of the Al_2O_3 carrier, the X1 and MEDC-B catalysts, the following metal-complex mechanism of the EOC catalysis on the surface of the mentioned catalysts can be suggested.

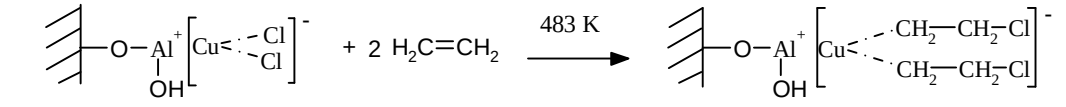

(11)

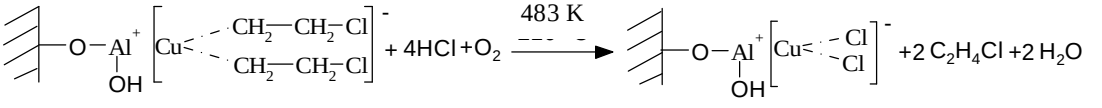

(12)

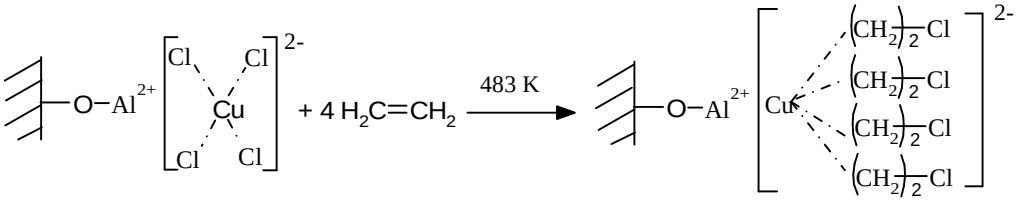

(13)

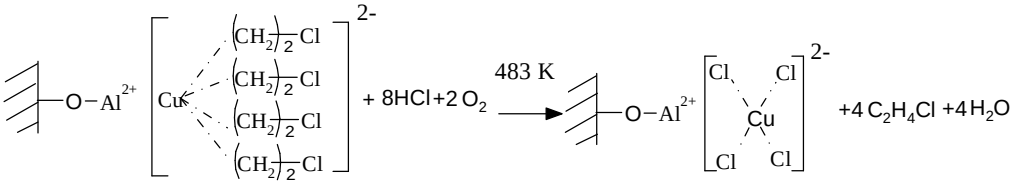

(14)

On the basis of EOC mechanism presented above and literature data indicating the existence of an independent $CuCl_2$ phase on the surface of EOC catalyst of the deposited type (X1) [12], as well as in the form of complex aluminate compounds of the $[CuCl_2]^{-1,-2}$ type [13], one can predict the catalysis mechanism as represented in Eqs. (11) and (12). And taking into account the fact that on the surface of the impregnated type EOC catalyst (MEDC-B) all the copper usually takes the form of complex $[CuCl_4]^{-2}$ compounds, which evenly interact with the surface groups of the support as shown in [11], we can predict that the prevailing catalysis mechanism will be as that represented by Eqs. (13) and (14).

The industrial use of these two different catalysts confirms above-described mechanism. The yield of 1,2-DCE is 1.5-1.7 times smaller on the catalysts of deposited type (X1) [17] compared with the impregnated type (MEDC-B), that is also evident from Eqs. (11)-(14). It is also known from the industrial practice that using the deposited type catalyst (X1) the ratio of the EOC reaction main reagents is $HCl:C_2H_4:O_2$ = (1.9–2):(1):(0.7–0.8), whereas using the impregnated type catalyst this ratio increases for hydrogen chloride and ethylene and decreases for oxygen – $HCl:C_2H_4:O_2$ = (2–2.2):(1–1.2):(0.5–0.6), which favors the increase in productivity of the main reaction of 1,2-DCE obtaining and the decrease of by-products yield, to calculate for one unit of the catalyst area. This is possible only in the case when the catalyst has a higher flow capacity, ***i.e.*** productivity by 1.2-DCE per 1 ton of the catalyst. As it was shown in [17], it increases by 1.5–2 times.

4. Conclusions

1. We have suggested the description of the active centres structure of the catalysts used for ethylene oxidative chlorination ($[CuCl_4]^{-2}$, $[CuCl_2]^{-1}$) on the

γ-Al_2O_3 support, namely of two types of catalysts: the deposited one (X1) and the impregnated one (MEDC-B). It has been shown that the interaction of $CuCl_2$ and the γ-Al_2O_3 surface groups (≡Al–OH) forms complex compounds with $[CuCl_4]^{-2}$, $[CuCl_2]^{-1}$.

2. We have developed a new mechanism of metal-complex catalysis of ethylene oxidative chlorination into 1,2-dichlorethane with the involvement of surface metal complexes $Al_2O_3[CuCl_4]^{-2}$, $Al_2O_3[CuCl_2]^{-1}$ reacting with ethylene, hydrogen chloride and oxygen.

3. It has been shown that under all other similar conditions the catalysts of impregnated type (Meds-B) are in 1.5–2 times more active and productive than the catalysts of deposited type (H-1) due to the differences in active centers structure and process mechanism.

Acknowledgments

This work was based on State program "Alternative technologies for 1,2-dichlorethane and vinylchloride with chlororganic waste recovery" (state registration number 0108U006570).

References

[1] Kurta S.: Khimiya i Tehnologiya Chlororganichnyh Spoluk. Plai, Ivano-Frankivsk 2009.
[2] Flid M. and Treger Yu.: Vinilchlorid. Himiya i Tehnologiya, v. 1. Kalvis, Moskwa 2008.
[3] Flid M.: DSc thesis, FGUP NII "Sintez", Russia, Mockwa 2002.
[4] Zolotovskii B.: DSc thesis, Novosibirsk, Russia 1992.
[5] Kurta S., Haber M. and Mikitin I.: Khim. Prom. Ukrainy, 2003, **55,** 9.
[6] Kurta S., Mikitin I. and Pronik O.: Pat. Ukrainy 24933, Publ. July 25, 2007.
[7] Kurta S., Mikitin I., Haber M. and Skakun P.: Pat. Ukrainy 88262, Publ. June 25, 2009.
[8] Mikitin I.: PhD thesis, Lviv, Ukraine 2009.
[9] Kurta S., Mikitin I. and Kurta O.: Fizika i Khimiya Tverdogo Tila, 2008, **9**, 577.
[10] Kulik T., Barvinchenko V., Palyanica B. *et al.*: Zh. Fizicheskoi Khimii, 2007, **81**, 88.
[11] Kurta S., Mikitin I. and Kurta O.: Fizika i Khimiya Tverdogo Tila, 2008, **9**, 143.
[12] Lamberti C., Prestipino C., Capello L. *et al.*: Int. J. Mol. Sci., 2001, **2**, 230.
[13] Jorgensen C.: Progr. Inorg. Chem., 1979**, 12**, 101.
[14] Garilli M., Fatutto P. and Piga F.: La Chimica e l'Industria, 1998, **80**, 333.
[15] Leofanti G., Padovan M., Garilli M. *et al.*: Int. J. Mol. Sci., 2001, **2**, 244**.**
[16] Leofanti G., Marsella A., Cremaschi B. *et al.*: J. Catal., 2001, **202**, 279.
[17] Kurta S., Mykytyn I. and Haber M.:Zh. Prikladnoi Khimii, 2005, **76**, 1110.

КАТАЛІЗ ПРОЦЕСУ ОКСИХЛОРУВАННЯ ЕТИЛЕНУ В 1,2-ДИХЛОРЕТАН ЗА УЧАСТЮ АКТИВНИХ ЦЕНТРІВ $CuCl_2$/CuCl НА ПОВЕРХНІ γ-Al_2O_3

Анотація. *На основі рентгеноструктурного аналізу носія γ-Al_2O_3 і каталізатора $CuCl_2$, CuCl на його поверхні, досліджена будова активних центрів. Показано вплив типу каталізатора на механізм процесу окислювального хлорування етилену. На основі даних мас-спектроскопічного аналізу вивчено різницю в будові активних центрів і механізмі роботи двох каталізаторів нанесеного й просоченого типу $CuCl_2$, $CuCl/\gamma$-Al_2O_3, в процесі окислювального хлорування етилену в 1,2-дихлоретан.*

Ключові слова*: процес, каталізатор, окислювальне, хлорування, спектроскопія, рентген, аналіз, центр, механізм, активність, продуктивність.*